Journal of New Materials for Electrochemical Systems

Vol.29, No.2, April, 2026, pp. 183-192

Journal homepage: http://www.newmaterials.ca/

Development of Superconductivity Technique Induced by Resonance for the Benefit of Thermal State of the Main Magnet Material Intended for Magnetic Resonance Imaging in Medical Use

Rachedi Mohamed [1*], Assas Oussama [2]

[1]Teacher researcher, Lecturer "A", Faculty of Technology, Department of Electrical Engineering , Laboratory of Electrical Engineering LGE , Dr. Moulay Taher Universty of Saida . Algeria

[2] researcher, Faculty of Technology, Department of Electrical Engineering, Industrial Electrotechnics, Dr. Moulay Taher Universty of SAIDA . Algeria

Corresponding Author Email: mohamed.rachedi@univ-saida.dz

https://doi.org/10.14447/jnmes/v29i2.a02

Received:
Accepted:

Keywords:
High flux Density, MRI, Magnetizing coil, Resonance technical, Superconductivity, Thermal stress optimization.

ABSTRACT

The talent for optimizing medical magnetic resonance imaging (MRI) equipment is crucial, especially in terms of cost, weight and volume. To date, the superconductivity technique dedicated to MRI has undergone a relaxation either for economic monopoly purposes, or maturity of research to find other more competing superconductivity alternatives. Two particularly antagonistic dilemmas were considered: generation of several Tesla, and reduced thermal stress threshold of the magnetizing coil. These constraints induced in the magnet main, generator of high magnetic field densities, constitute inevitable challenge to be faced, despite the varieties of cooling solutions adopted, and put into service being. In this regard, a new contribution to relieve the heating occurring an MRI system is at the heart of this investigation. This option is mainly based on strategy for developing a new power supply for generator with high MRI density magnetic, assisted by the resonance technique. This alternative procedure involves switching the converter's semiconductors at frequencies close to the resonant frequencies of the passive components, specifically the magnetization circuit and the compensation capacitor, which are selected for each flux density used. Furthermore, this frequency range will maintain the properties of the main magnet materials in a normalized thermal state, given that power losses are optimal, well before magnetic saturation. This solution will allow the availability of high-voltage capacitors, which are highly recommended for this type of medical equipment.

NOMENCLATURE

R	specific internal coil rsistance, Ohm
R_i	iron resistance magnetizing circuit, Ohm
L	coil inductance , Henry
L_m	Main magnetization inductance, Henry
L_f	leakage r inductance, Henry
X_f	leakage reactance, Ohm
X_m	reactance magnetization, Ω
X_{LR}	coil reactance in resonance mode, Ω
X_{CR}	capcitor reactance in resonance mode. Ω
Cp	Parasitic capacitore, pF
I_{CP}	stray current, mA
B_0	main density magnetic field, Tesla
I_m	manetization current, A
I_0	parasitic branch current, mA
w_0	normal operating pulsation, rd.s^{-1}
f_0	normal operating frequency, Hz
w	resonance pulsation, rd.s^{-1}
f	Resonance frequency, KHz
$\|Z\|$	impedance magnitude

Greek symbols

Ω	Resistance Ohm unit
ϱ	damping system
ϕ	Magnetic flux, Weber
μ	magnetic permeability, Hm^{-1}
Δu	voltage difference

Subscripts

MRI	magnetic resonance imaging
EMC	electromagnetic compatibility
PWM	Pulse widh modulation
HF	high frency
He	Liquid Helium

1. INTRODUCTION

The technique of medical imaging is mainly known as the means of clinical investigation most used by the human health sector. This attractive field has continued to progress, given its vital aspect which called upon several disciplines, thus the therapeutic and diagnostic trends have strongly launched very advanced research in order to further regulate the human health sector. Medical imaging by magnetic resonance (MRI) has been dedicated to global health as a new cutting-edge alternative. The contributions already valued for the benefit of this imaging technique, have made the fertile field of investigations to further relieve the health sector to a more comfortable state in terms of increased diagnostic precision.

To generate a high density magnetic field, a strongly pulsed current with high amplitudes will be recommended. However, the resistance parameter of the gradient coil is a limiting factor in the face of the thermal constraints which manifest strongly at the heart of the main magnet. To cope with this major constraint, it is recommended to use a superconducting magnet, with the winding material emerged in a special cooler, having the ability to align the thermal characteristics of the magnetizing coil wires to a near resistance of the zero value.

Thus, magnetic fields of several Teslas can be obtained by using windings of several turns of superconducting wires immersed in liquid helium, often based on alloys of Niobium and Titanium (NbTi) or Niobium and Tin (Nb3Sn) [3]. These coils are often called “superconducting magnets”.

In this context, three major parameters are fundamentally discussed in this type of equipment:

- The critical current, through the coil to maintain its superconductivity.
- The critical field, this is the maximum magnetic field that can be applied to a superconducting material.
- The disadvantage of superconducting Helium is accidental transformation from liquid to gaseous state.

It is necessary to report the harmful emissions generated when a quench occurs [6-9]. Thus, potential economic losses are heavily estimated when the system is put back into service.

To deal with these disadvantages, an approach has been developed whose objective is to obtain a high-density magnetic field MRI generator, assisted by the superconductivity induced by the resonance technique. This method could be an alternative to the currently adopted uncompetitive superconductivity, which is achieved by equipment still considered cumbersome, heavy and very expensive.

This technique is only obvious when the resonance phenomenon caused by the energy reservoir correctly identified by the inductance of the coil of the magnetic MRI inductor and the integrated capacitor accordingly. However, no over voltage will be imposed on the edges of the load during this resonance. Thus, a variety of loads can be implemented, where the switches in the designated DC-AC converter will be subjected to other new frequency ranges of switching, assigned by resonance of the passive elements specific to each typically severed load.

2. PRINCIPLE AND CHARACTERISTICS OF THE MAIN MAGNET IN MRI SYSTEM

The main field magnet is designed to exacting specifications, but manufacturing, installation and usage challenges require additional tools to assign target performance. for these considerations, the elements for the design of the magnetic circuit have been fully taken into account, given their interactions in the frequency domain.

The main magnet of an MRI system provides a strong, homogeneous and stable B_0 field required for medical magnetic resonance imaging use.

Permanent magnets or resistive electromagnets are typically used for whole-body MRI scanners with $B_0 \leq 0.4$ Tesla, while superconducting magnets generate higher field strengths $B_0 \geq$ 1.5 Tesla for medical imaging use by magnetic resonance. The magnetic field in the solenoid coils is given in formula 1 and formula 2 for a magnetizing coil.

$$B = \mu.\frac{N}{l}.I \tag{1}$$

$$B = \frac{0.8991.10^{-6}}{r}.N.I \tag{2}$$

For the design of magnetizing coils, the following criteria must be respected:

- The coil must be designed for the capacity to manage highly pulsed currents from a heating point of view.
- Ensure that the self-resonance frequency of the coil is five to ten times higher than the working frequency [8].
- Adjust the coil radius as small as possible to optimize its impedance and parasitic capacitor.

Design the coil to favorably manage high voltage (avoid electric arcing).

2.1 ADOPTED MODEL OF HIGH MAGNETIC FIELD GENERATOR

In order to obtain an electrical model of the magnetizing coil it is initially necessary to consider the main elements which contribute to the inductor circuit of the main magnet. The parasitic elements were also considered to establish the following equivalent circuit designed bay figure 1 that shows the simplified equivalent circuit of a real inductor whose elements are defined as follows:

- R: the resistance resulting from the winding wire;
- L: the inductance of an ideal coil;
- R_i: Resistance represents the heating in the iron of the magnetic circuit.
- C_P: the coil parasitic self-capacitor and its terminations.
- L: the overall inductance of the coil and X_L its own reactance.

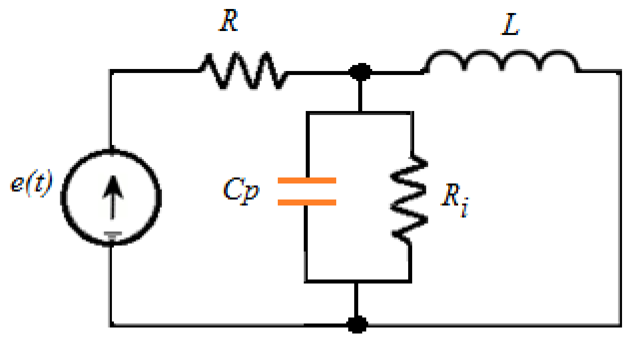

Figure1. Equivalent circuit of solenoid coil with iron core

In the case of high frequencies, it is impossible to ignore theparasitic capacitor reactance which can be quite significant, in fact, to be able to reduce this inconvenience; various winding techniques are within the reach of the manufacturer. Increasing the number of turns also increases the parasitic capacitance *Cp*. And then, higher *Cp* reduces the self-resonance frequency of the coil. The coil circuit representing the main field magnet is shown in figure 2, of which the following elements are defined as felow:

– L_m: Main coil inductance, and X_m; its reactance.
– L_f : leakage inductance of coil, X_f; its leakage reactance.
– I_m: Main current of coil and I_0 : Leakage current of the parasitic capacitor.

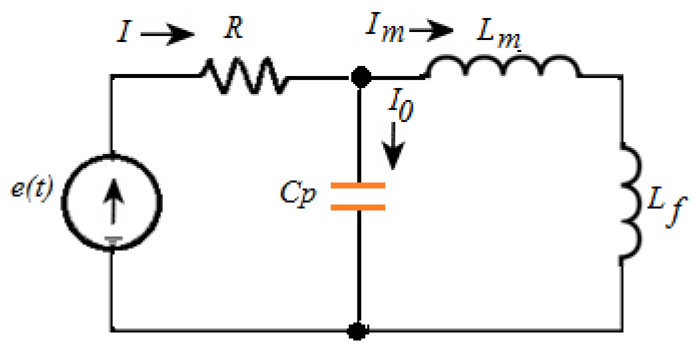

Figure2. Self-resonance of intrinsic inductor circuit coil and parasitic capacitor included, with area core

$$X_L = w.L \tag{3}$$

$$X_{Cp} = \frac{1}{w.Cp} \tag{4}$$

$$I_m = \frac{V}{R + j.L.w} \tag{5}$$

$$I_0 = j.C_p.w.V \tag{6}$$

With, $w=2\pi f$, the circuit's own pulsation, I_0 parasitic current and I_m magnetizing current.

2.2 INTRINSIC SELF-RESONANCE MODE OF MAGNETIZING COIL

As shown in figure 2, the equivalent circuit adopted for the magnetizing coil equipped with the parasitic capacitance Cp, thus the expression of the equivalent impedance of this main magnet allows you to obtain formula 7 describes the modulus of this impedance. Given that for the practical case, the internal resistance is infinitely small, whose inverse proportionality as a function of the frequency on the two members in the denominator, allows two antagonistic cases to be deduced:

- At low frequencies, the branch *w.Cp* behaves short circuit, and that ($R+1/wL$) behaves as an open circuit.
- At high frequencies, the branch w.Cp behaves open circuit, and that (R+1/wL) behaves as a short circuit.

$$|Z_0| = \frac{1}{\sqrt{R^2 + \frac{1}{w^2L^2} + w^2Cp^2}} \tag{7}$$

$$w_0 = \frac{1}{\sqrt{LCp}} \tag{8}$$

Thus $$f_0 = \frac{1}{2\pi\sqrt{LCp}} \tag{9}$$

And $$C_P = \frac{1}{2.\pi\sqrt{L.f_0}} \tag{10}$$

With: $w_0=2\pi.f_0$, the frequency f_0, represents the self-resonance frequency specific to the coil considered.

The second variant (high frequency case) offers the opportunity to choose operating frequencies favorably suited to block the leakage current of the parasitic capacitor on one side, on the other side to allow an almost total absorption of the current through the magnetizing coil circuit. Consequently, the identification of the self-resonance of the inductor circuit is a determining factor for the design of main magnet coils in MRI application. Formula 10 shows the effect of high self-resonance frequencies to eliminate the influence of the parasitic capacitor C_P. This particularity requires the design of coils generating high magnetic field intensities, with self-resonance at hyper frequencies. Thus, two advantages will be acquired:

- Infinitely small parasitic capacitor reactance.
- Provide system operating frequencies, highly spaced from self-resonance

The results shown in Table 1 identify the range of self-resonance frequencies not to be exceeded or overlapped, especially below the permissible threshold value. This frequency indicates the practically adopted value of the parasitic capacitor current. A high self-resonance frequency of an inductor circuit, provided with a parasitic capacitor C_P, will unfavorably limit the maximum working frequency of the coil.

Table 1. Validation of the model conforming to the inductor coil

R Ω	L µH	X_L m Ω	C_P pF	X_{Cp} m Ω	f_0 MHz	I_L A	I_{CP} mA
0.25	**5**	**1.88**	**2**	**1.33**	**50.33**	**63**	**0.00**
0.35	7.5	2.82	5	0.53	25.99	58	0.08
0.45	10	3.77	10	0.27	15.91	49	0.15
0.55	12.5	4.71	15	0.18	11.62	37	0.25
0.65	15	5.65	20	0.13	9.18	25	1.25
0.75	17.5	6.59	25	0.10	7.60	17	5.25
0.85	20	7.53	30	0.88	6.49	12	12.50
0.95	22.5	8.48	35	0.75	5.67	6	17.25
1.05	25	9.42	40	0.66	5.03	2	25.15
1.15	**27.5**	**10.37**	**45**	**0.59**	**4.52**	**1**	**28.32**

3. TECHNICAL FOR ACTIVATING COIL SUPERCONDUCTIVITY BAY RESONANCE

After consulting the characteristics of the resonant tanks, and their different combinations, the topology with two resonant elements adopted was that of series resonance (SR). At the resonant frequency, the impedance of the series-connected resonant elements becomes zero and then, input-output gain is unity. Therefore, SR performs a function as a buck converter. Thus, the tanks of the L_R-C_R couple are really resonant converter candidates.

Figure 3 shows the compensation by integrating a resonance capacitor to counterbalance the overvoltage arising across the terminals of
the superconducting coil inductance. Therefore The module of this impedance is given by formulas 11, when the capacitos must be chosen adequately, to ensure it acts as a component causing the cancellation of the overall impedance of the magnetizing circuit during resonance.

In light of previous results (Table 1), the resonance frequency range selected for the L_R-C_R series tank must be strictly five to ten times higher than the anti resonance frequency range. Hence, this characteristic will make it possible to exclude interference from parasitic capacitors, when operating the magnetizing system outside frequency categories.

$$|Z_R| = \sqrt{R^2 + \left(wL_R - \frac{1}{wC_R}\right)^2} \qquad (11)$$

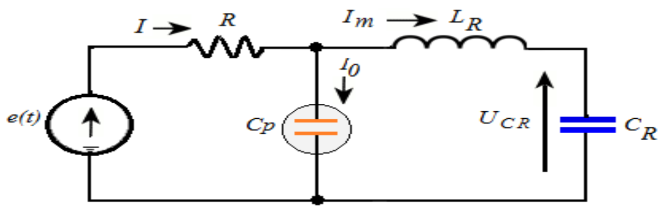

Figure 3. Equivalent circuit adopted with series-resonant, SR LR-CR tanks

3.1 ZERO VOLTAGE POWER SUPPLY STRATEGY BY SERIES RESONANCE MODE

Once the resonance condition occurs, the polarity change of over voltages of passive components is established. Therefore, the reactance of the capacitor is the same as the coil's reactance at a given resonance frequency, as stipulated in formula 12, including f_R resonance frequency and knowing that Q is the load factor.

$$C_R = \frac{1}{(2.\pi.f_R)^2.L_R} \qquad (12)$$

$$Q = \frac{1}{R}\sqrt{\frac{L_R}{C_R}} \qquad (13)$$

The formula 12 allows to calculate capacitor values as a function of resonance frequency, the results shown in Table 2 clearly show that it is possible to activate superconductivity for the benefit of the main magnet, generator of high magnetic field intensities under absolutely reduced voltage. Indeed, for different pairs of resonant circuits, the assumed fixed inductance with variants of capacitors which are integrated, put into service, it results that the X_{LR} and X_{CR} reactances are strongly flashed under high frequencies.

Therefore, for each of the operating frequency that aligns the resonant frequency specific to each variant (L_R-C_R), the equivalent impedance reactance of the circuit in question remained infinitely small.

Knowing that the main magnet inductance chosen for L=5 H with its internal resistance R=0.5. The ratio of the auto-resonance frequency to the operating frequency of the magnetizing generator must be strictly greater than or equal to ten and that, to neutralize the auto-resonance effect of the coil on the dynamic characteristics of the power supply system and the installation parameters.

$$u_{CR} = \frac{1}{w_R.C_R} = I.w_R.L_R \tag{14}$$

Figure 4 shows the variations in the maximum voltage u_{CR} at the terminals of the capacitor considered as a regulator, which limits the voltage at the terminals of the overall impedance of the load to the value U_R, once the following condition is met.

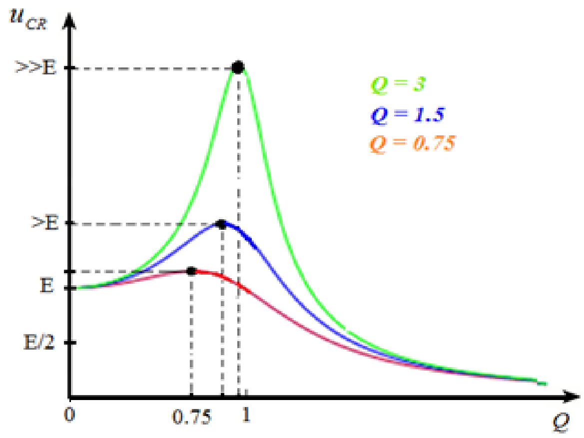

Figure 4. Profile of capacitor voltage CR Variations as a function of the quality

Table 2. Activation of superconductivity in magnetizing generator by the resonance technique

f_R kHz	C_R pF	X_{LR} Ω	X_{CR} Ω	Z_{LRC} Ω	U_{CR} V	U_R V	I_{LR} A	Q
5	22.50	0.16	1.31	**0.25**	380	8	12	1.88
15	8.10	0.78	1.55	**0.87**	510	14	19	3.14
25	4.10	1.10	1.82	**0.80**	750	21	28	4.41
35	2.50	1.41	2.21	**0.83**	885	27	37	5.65
45	1.60	1.73	2.41	**0.73**	960	32	43	7.07
55	1.20	2.04	2.72	**0.72**	18000	43	54	8.16
65	0.90	2.35	2.35	**0.26**	21000	49	62	9.42
75	070	2.67	2.67	**0.25**	25000	57	75	10.20
95	0.56	2.98	2.99	**0.25**	31000	61	84	11.25
105	**0.46**	**3.30**	**3.29**	**0.25**	**37000**	**80**	**90**	**1.17**

3.2 RESONANT BUCK CONVERTER USED FOR ACTIVATING SUPERCONDUCTIVITY

The main field magnet used in magnetic resonance imaging equipment, is manufactured to rigorous specifications, but the challenges of realization, installation and use, require additional tools to maintain operational performance targets.

MRI, which is based primarily on the interactions between nuclear magnetic moments and applied magnetic fields, uses a range of electromagnetic (EM) tools to optimize all magnetic fields necessary for image production.

Therefore, it is advisable to cover the performance dependent on electromagnetic computer modeling to offer a cost-effective contribution to the benefit of this equipment.

As condition strictly respected, the self-resonance of the magnetization coil must in no case encroach on the effect of the resonance technique in question, hence the parasitic capacitor C_p will be negligible compared to the integrated high voltage capacitor C_R.

In terms of new materials used in the main magnet, its behavior under high frequencies offers improved performance; indeed, power losses in the chosen magnet are optimal, well before its magnetic saturation [2], [7]. Thus, these qualities correspond to an optimal magnetic flux density.

Since the RLC series circuit is subject to a voltage step E, the relations deduced from the mesh law can be described as follows:

$$e(t) = u_R + u_{LR} - u_{CR} \tag{15}$$

By introducing the characteristic relation of the capacitor designated as a regulator, this is governed by the differential equation of the second order system:

$$e(t) = R.C_R.\frac{du_{CR}}{dt} + L_R.C_R.\frac{d^2u_{CR}}{dt^2} + u_{CR} \tag{16}$$

$$i = C_R\frac{du_{CR}}{dt} \tag{17}$$

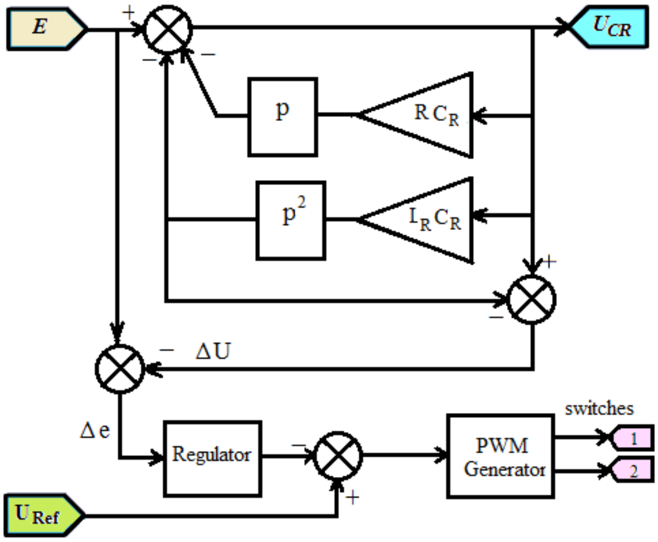

Figure 5.functional block diagram corresponding to a phase

Modeling the passive circuit by introducing the operator, *p= d/dt* gives the following representation:

$$U_{CR} = E \; - R.C_R.p.U_{CR} - \; L_R.C_R.p^2. \;\; U_{CR} \tag{18}$$

Mainly, the activation of superconductivity is limitedly subordinated to the voltage states of the high voltage integrated capacitor, as follows:

$$\begin{cases} U_{CR} = U_{LR}, U_R = E \\ U_{CR} > U_{LR}, U_R = E - \Delta u \\ U_{CR} < U_{LR}, U_R = E + \Delta u \end{cases} \tag{19}$$

- ∗ If U_R =*E*, the system is inside relative superconductivity.
- ∗ If U_R >*E*, the system is inside relative superconductivity.
- ∗ If U_R <*E*, the system is outside superconductivity.

With:

- – Δu: voltage difference
- – *E*: voltage generator, in volts (V);
- – u_{CR}: voltage at the capacitor terminals, in volts (V);
- – L_R: inductance of the coil, in henrys (H);
- – i: current in the circuit, in amperes (A);
- – C_R: electrical capacity of the capacitor, in farads (F);
- – R: magnetizing coil resistance, in ohms (Ω);
- – t: time in seconds (s).

The assumption here is that the RLC circuit, governed by equations systems 19, are perfectly linear. The two quantities whose derivative is involved are current i and voltage u_{CR} at the terminals of the capacitor C_R. As shown in Figure 6, including downstream assistance from a pulsed current source, which controls the intensity of the electrical current delivered into the coil. Thus, high field intensity at high frequency is obtained by using a resonance capacitor to cancel the impedance of the coil.

The current amplifier, which in this application is more often called in the occurrence; switching power supply, which, has been assigned to it the control of the intensity of the electric current delivered in the magnetizing coil. As shown in Figure 6, when a high frequency magnetic field is required, the resonance technique will reduce the coil impedance which will allow for high current driven by a low voltage function generator amplifier.

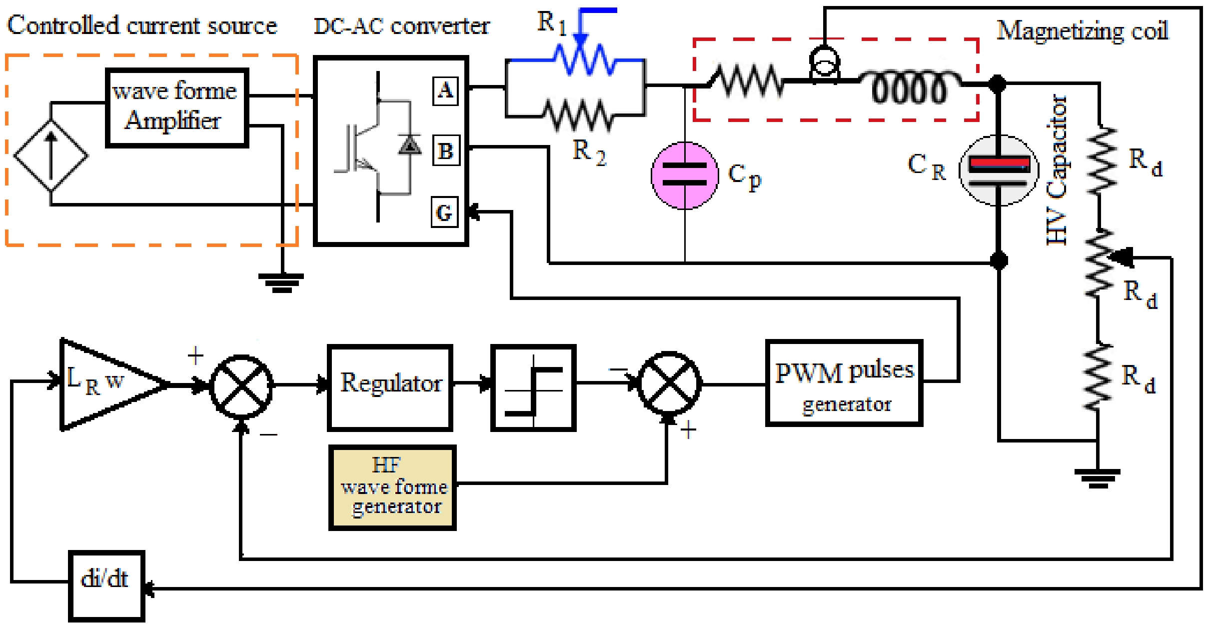

Figure 6. Schematic of the assembly combined with controllers to manage thermal optimization of systeme magnetizing

4. CHARACTERISTICS OF HIGH MAGNETIC DENSITY GENERATOR BY EXITATION

During the excitation of the main magnet generating high magnetic field densities, an adaptable voltage capacitor was properly selected. Assuming that the load parameters were selected accordingly, then a variety of voltage regulator capacitors have been put into service for each case and those, to activate the superconductivity induced by electrical resonance of passive energy storage elements. To obtain the most efficient response qualities, two types of controllers (PID and Fuzzy logic) have been set up. Respecting the strict conditions of spacing between the coil's own auto-resonance frequency and that of the primary circuit's resonance, it is evident to effectively neutralize the influence of the coil's intrinsic CP parasitic capacitor on the desired operation of the assembly in question.

This feature has been actively tested experimentally. To give concrete expression to this approach, a parasitic current threshold has been adopted whose relation with the main current is ideally negligible, and this in accordance with the predetermined relation between the auto-resonance frequency and that of the main passive circuit.

4.1. POWER SUPPLY, MANAGED BY PID CONTROLLER MEDIUM LOAD CASE

Figures 7.a and 7.b shows a perfectly uniform reduced voltage at the main circuit terminals. In reality, this reduced voltage is only the one at the terminals of the internal resistance of the magnetizing coil generating high magnetic field densities.

However, large amplitudes of pulsed currents can be injected into the magnetizing coil under superconductivity conditioning, which is announced during the resonance phenomenon. Therefore, the thermal stresses at the heart of the magnetizing circuit are increasingly optimized. This important feature is clearly shown in Figure 7.c.

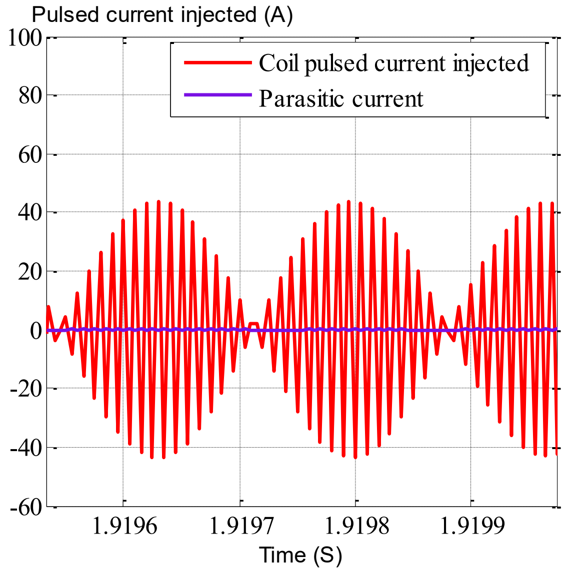

Figure 7.a. pulsed current injected into the main magnetizing coil at medium power

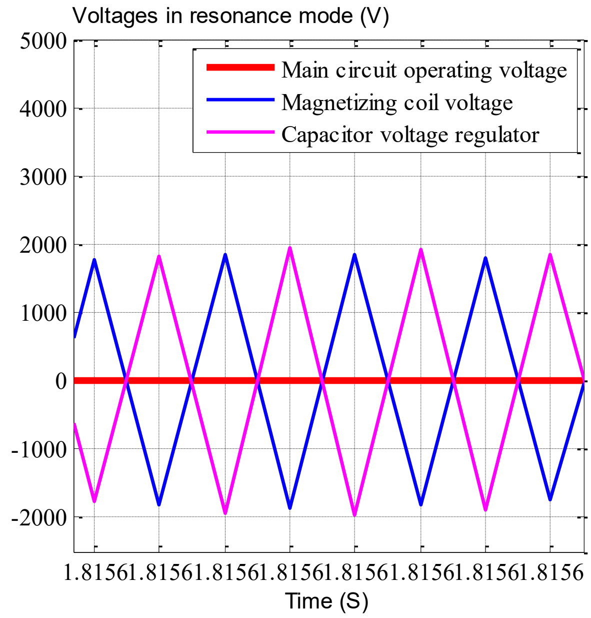

Figure 7.b. Profile of resonance technique contribution to activate superconductivity in main magnet

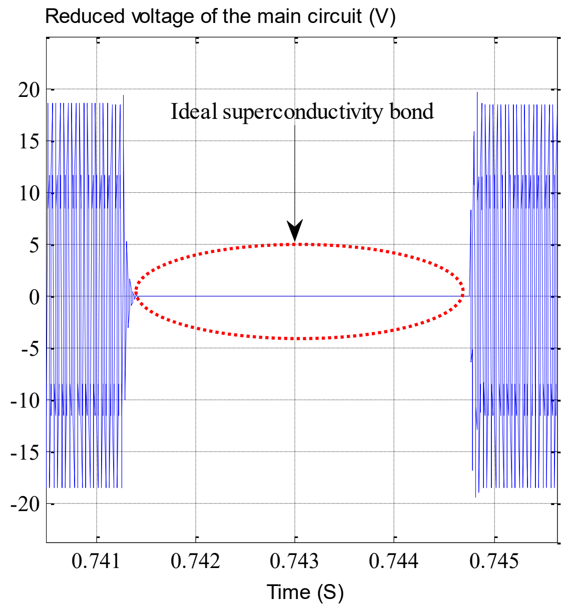

Figure 7.c. Uniformly reduced voltage of the entire inductor circuit, in full current

4.2 POWER SUPPLY, MANAGED BY THE PID CONTROLLER HEAVY LOAD CASE

As shown in figures 8.a and 8.b for each charge absorbing high intensities of pulsed currents, a suitably chosen capacitor reactance as voltage regulator has been assigned to it. In such circumstances, the results obtained in these figures, where the voltages announced by these capacitors during their resonance mode did not exceed critical values, which correspond to oversized passive elements.

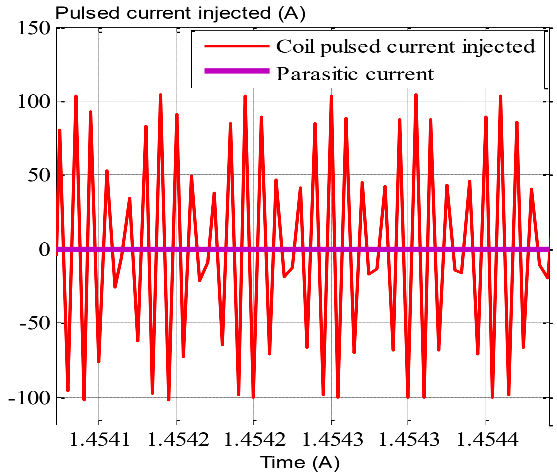

Figure 8.a. Pulsed current injected into the main coil at heavy load power

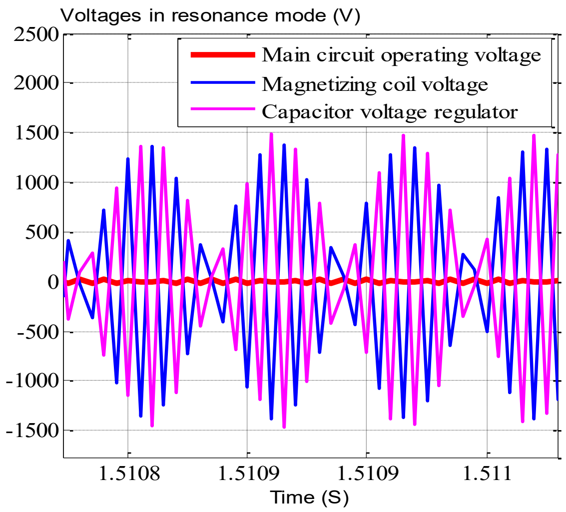

Figure 8.b. Resonance technique contribution to activate superconductivity in main magnet

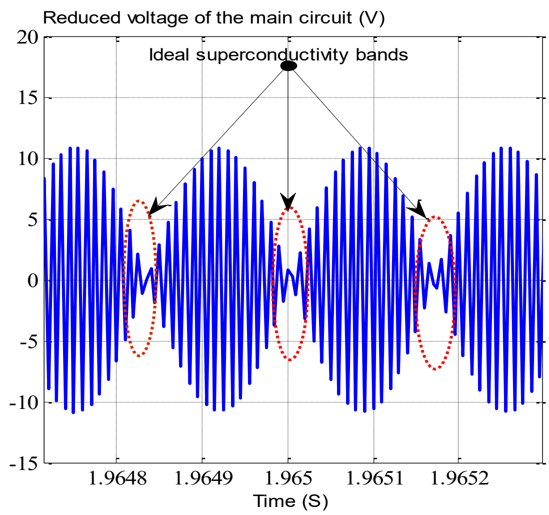

Figure 8.c. Uniformly reduced voltage of the entire inductor circuit, in full current

In addition, no requirement to exceed the standard values of the available contracts for this type of capacitor. On the other hand, whatever the load identified to embrace the resonant series circuit for set up, the voltage of the capacitor will not exceed 20 kV. In this case, the current absorbed by the coil is strongly conditioned by controlling the resistor voltage that represents the thermal seat of the main magnet (Figure 8.c). In the light of these results, there will be no concern for the availability of standard high voltage capacitors, and a large number of heated trips have been made, indeed, the optimization of thermal stress accumulation in the inductor circuit is imminent. These characteristics are considered crucial for the benefit of MRI equipment intended for medical imaging.

4.3 POWER SUPPLY, MANAGED BY THE FUZZY LOGIC-PID HYBRID CONTROLLER

Certainly, the inadequacies of control of the transient regime previously managed by the PID controller of the system representing magnetic flux density generator has been the object of questioning this technique. Where the use of other alternatives for solutions perfectly adequate to these kinds of constraints is strongly solicited. In this investigation, a reflection was suggested to consolidate the foundation of the contribution of this technique. The hybrid hybrid fuzzy logic-PID controller strategy has been tested to idealize the profiles of the results already obtained by the PID controller.

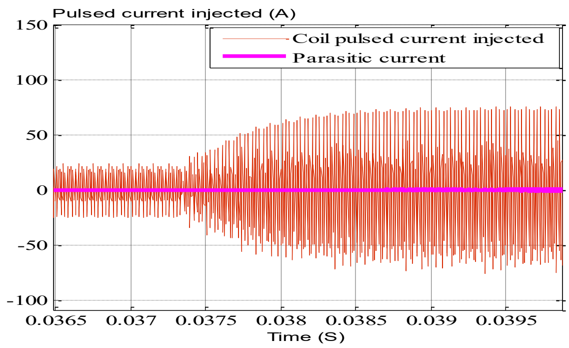

Figure 9.a. pulsed current profil injected into the main magnetizing coil at medium power

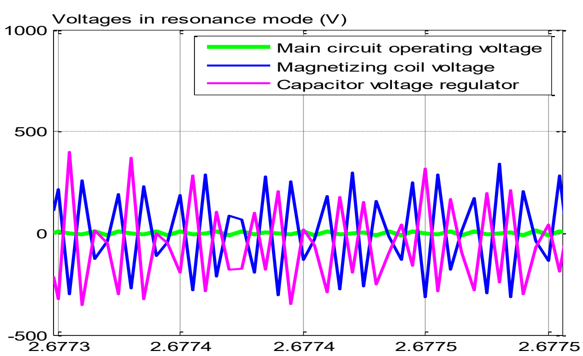

Figure 9.b. Profile of resonance technique contribution to activate superconductivity in main magnet

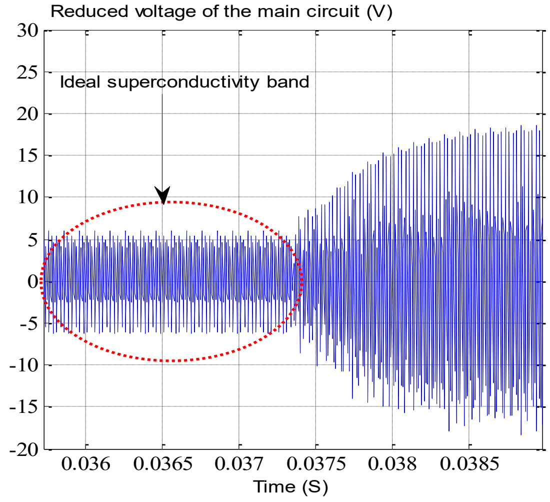

Figure 9.c. Uniformly reduced voltage of the entire inductor circuit, in full current

4.4 DISCUSSIONS AND INTERPRETATIONS

Using the hybrid controller, the results obtained provide performance translated into system control, whether in dynamic mode or static mode. Compared to the fuzzy logic controller assistance, the transient overshoots are perfectly damped; hence the power supply of the magnetizing circuit under much more optimized thermal constraints will be achieved. These features have been illustrated in the figure 9.a. At resonance, the voltage profile across the load as shown in figures 7.c, 8 .c and 9.c which indicates the ideal superconductivity band and the relative superconductivity band. This results in a mean operating voltage that is favorably conditioned for the injection of high current amplitudes, necessary for magnetic resonance imaging applications**.** Initially, the magnetizing coil with suitable capacitor is subjected to a perfectly uniform voltage with an amplitude of 0 to 5 Volts, however (figure 9.c), a charge current is strongly injected without excessive thermal stress, which then allows to increase the dose in field density of the main magnet for the rest of time, necessary for the generation of high magnetic field densities.

5. CONCLUSION

In this investigation, a superconductivity priming strategy was tested for the main field gradient coil, which is designated for medical imaging MRI supply. High reliability of the resonance of the passive circuit of the system, whose main inductor is associated with a compensation capacitor favorably adapted to trigger superconductivity. However, an appropriate adjustment of the switching frequency of the semiconductor components of the inverters put into service to overlap the resonance frequency of the global passive circuit. This option of technicality has largely favored the excitation of the magnetizing coil by strongly pulsed currents in order to generate desired and rated magnetic flux densities. At the same time, a possibility of extending the range of high-voltage capacitors which has promoted the opportunity of recourse to this technique of resonance, which will be able to circumvent the concern for superconductivity.

Therefore, an upcoming standardization methodology of the compensation capacitors integrated in these types of equipment has been adopted to relieve the modern medical imaging market. In addition, the foundation of this approach on the basis of the obtained results will allow the realization in real time of the activation of superconductivity by the resonance technique. Thus, thermal optimization of the generator enclosure at high magnetic flux densities may be able to compete with the power supplies of this type of MRI equipment, which are until now exclusively assisted by coolers, heavily supported on the economic and safety level, such as liquid Helium at very low temperature in association with Barium Titanate. Even though MRI has already reached a certain maturity, it is certain that new developments and alternatives are to be expected as stipulated in this contribution.

REFERENCES

[1] M.Brix, M. K.Ersland, L.Hugdahl, K.Grüner, " Brain MRI Spectroscopy in Autism Spectrum Disorder the GABA, Excitatory/Inhibitory Imbalance Theory Revisited Frontiers in Human Neuroscience, " 2015, vol. 9, pp.365, doit:10.3389/fn hum.

[2] Rachedi Mohamed, Mohamed Chikouche Tarik, "Development of Control Strategy for Power Supply to Optimize Thermals Effects Induced in X-rays Tube for Medical use," Dec. 2018, ICCEE, vol. 25, no. 4, pp. 1087-1099, doi.org/10.1080/02841860802244158.

[3] Steve Webb, " The Contribution, History, Impact and Future of Physics in Medicine, Acta Oncologica, " British medical physicist and writer, professor of physics at the Joint Department of Physics 2009, vol.3, pp.169-177 ,ISSN 0284-186X, doi.org/10.1080/02841860802244158

[4] Robert A. Pooley, AAPM/RSNA, "Physics Tutorial for Tesidents: Tundamental Thysics of MRI Imaging, Radiographics," Jul-Aug. 2005, vol. 25, no. 4, pp. 1087-1099, https://doi.org/10.1148/rg.254055027.

[5] M. Rachedi , M. Bourahla, "Optimization strategy of distortion rate control for high power transfer supplying an x-ray tube," JEE, March. 2012, vol.63, no.2, pp. 81-87. doi.org/10.2478/v10187-012-0012-z.

[6] Mc.Robbie, " MRI From Ficture to Froton, " Nov 2003, vol. xi, pp. 359.

[7] Rachedi Mohamed, Bouanane Abdelkrim, " Stratégie de contrôle hybride pour l'optimisation des contraintes thermiques cumulées induites dans un tube à rayons X à usage médical," Oct. 2019, I IJECE, vol. 9, no. 5, pp. 3944-3955, doi.org/10.1080/02841860802244158.

[8] Certaines and Cathelineau, "Safety Rspects and Ruality Rssessment in MRI and MRS: a Rhallenge for Realth Rare Rystems in Europe, J Magnetic Resonance Imaging," Apr. 2001, vol.13, no.5, pp. 632-638, https://doi.org/10.1002/jmri.1089.

[9] K.Baker, B.Tkach, J.A.Nyenhuis, J.A.Phillips, M.Shellock, G.Martinez, "Evaluation of Spécific Absorption Rate as a Dosimeter for MRI-Related Rmplant Reating Magnetic Resonance Imaging," 2004, vol. 20 no. 2, pp. 315–320,doi.org/10.1002/jmri.20103.

[10] A.Haocke, E. Mark, D.Brown, C.Roberts, K.Thompson, B.Vankatesan, " Magnetique Resonance

Imaging Physical Principals and Sequence Design, " New York, J.Wiley & Sons 1999.
[11] Wendell A. Gibby, " Basic Principles of Magnetic Resonance Imaging," Neurosurgery Clinics of North America, Jan 2005, vol. 16 no. 1, pp. 1-64, https://doi.org/10.1016/j.nec.2004.08.017.
[12] P.Jannin, C.Grova and B.Gibaud , " Fusion de Données en Imagerie Médicale, " revue méthodologique basée sur le contexte clinique, ITBM-RBM, 2001, vol. 22 no.4, pp. 196-215, https://doi.org/10.1016/s1297-9562(01)90049-x.
[13] DW.Townsend and T. Beyer, " A Combined PET/CT Scanner: the Path to True Image Fusion, " British Journal of Radiology 2002, vol.75, pp. S24-S30, https://doi.org/10.1259/bjr.75.suppl_9.750024.
[14] Bruno Van Oystaeyen : Physicist UCL 1973, Doctor of Science UCL 1978, Retired lecturer at HELHa, Haute Ecole Louvain en Hainaut.
[15] J.Fourier , " Le Mouvement de Protéines Essentielles a la Vie d'une Cellule Filmé Pour la Première Fois, " Communiqué du 9 Octobre 2012 frome Joseph Fourier University .
[16] A.Etevenon, "Étude Méthodologique de L'électroencéphalographie Quantitative, Application à Quelques Exemples, " State doctoral thesis in natural sciences, Nov 29 1977, Pierre et Marie Curie University, Paris, pp.303, Copédith, Paris, 1978.
[17] Ordidge, Kanal, " special issue: MR safety. J Magn Reson Imaging, " 2000, vol.12, pp.1-204.
[18] F.Kerviler, A. Bazelaire, " Risks Associated with MRI: Safety Rules, Incidents, and Accidents, "Journal of radiology, May 2005, vol. 86 and no.5, pp. 573-8, https://doi.org/10.1016/s0221-0363(05)81410-6.
[19] D.Sarrut , " Recalage Multimodal et Plate-Forme d'Imagerie Médicale à Accès Distance, " Doctoral Thesis, University of Lyon 2, 2000.
[20] Shellock, "MRI Safety, Bioeffects and Patient Management, " May 8 2007.
[21] Zhuo, Gullapalli, " AAPM/RSNA Physics Tutorial for Residents: MR Artifacts, Safety, and Quality Control, Radiographic, " Jan-Feb 2006, vol.26 no.1, pp. 275-97.
[22] Elwe Didactic GmbH, " Steinfelsstrasse 6. 08248 Klingenthal, " www.elwedidactic.com, 38 Scientific GmbH Rudorffweg, B.21031 Hambourg, Germany.
[23] J.Angel, M.Garcia, P.Blanc , " Design criteria for transformer sin high voltage output, high frequency power applications, " EPE5, Jun 1994, pp. 125–132, https://doi.org/10.1080/09398368.1994.11463354.
[24] J-P.Dillenseger, M.Elisabeth , "Guide des technologies de l'imagerie médicale et de la radiothérapie," Quand la Théorie Eclaire la Pratique, édition Masson, 2009, pp. 111.
[25] C.M.Liu, W.Swift, B.J.,and M.B.Smith, " Combination of Optimized Transmit Arrays and Some Receive Array Reconstruction Methods Can Yield Homogeneous Images at Very High Frequencies Magn Reson, " 2005 Collins, vol. 54 no. 6, pp. 1327–1332. https://doi.org/10.1002/mrm.20729.
[26] W.Salameh , " Imagerie par Résonance Magnétique Nucléaire pour la Vélocimétrie d'un Ecoulement en Milieu Poreux , " Thesis Defended 2011, Ecole Doctorale, Energie Mécanique Matériaux, Laboratoire d'énergétique et de Mécanique Théorique et Appliquée.